Trial of Point Cloud Registration Method at Excavation Sites and Implementation of Machine Guidance System

Kai Sato[1], Takashi Yokoshima[1], Yuki Miyashita[1], Aoi Tarutani[1], Keisuke Imoto[1], Fuku Himuro[1], Yutaro Fukase[1], Yusuke Nishida[2], Yusuke Shibata[3], and Toshiki Aizawa[3]

[1]Institute of Technology, Shimizu Corporation, Japan
[2]Tokyo Civil Engineering Division, Shimizu Corporation, Japan
[3]East Nippon Expressway Company Limited, Japan
sato_k_213279@shimz.co.jp

Abstract–

Machine guidance using total stations (TSs) and global navigation satellite systems (GNSSs) is implemented to reduce labor and improve productivity in excavation work. However, a challenge with existing methods is that obstacles can interfere with guidance. Direct measurement of excavation surfaces using LiDAR can solve this problem, but it requires a point cloud registration method capable of functioning even in feature-poor environments, such as tunnels. We developed a registration method that can be used feasibly in excavation sites and built a system that visualizes the excavation status using LiDARs. The proposed robust registration method utilizes a specialized jig and a TS, specifically designed for feature-poor excavation sites. The system achieved a measurement accuracy of ±20 mm in field trials, satisfying the requirements set by site staff (±50 mm in every 250-mm pitch and a refresh rate of <30 s) and overcoming the limitations of conventional TS/GNSS methods in tunnel environments.

Keywords

LiDAR; Point cloud; Machine guidance

1 Introduction

To improve productivity in response to construction labor shortages [1], researchers have proposed machine guidance (MG) for presenting the excavation status to operators and machine control (MC) for autonomous excavation [2]–[4]. Systems detecting heavy machinery positions using global navigation satellite systems (GNSSs) or automatic-tracking total stations (TSs), and systems estimating boom and bucket postures via tilt sensors, are already being used in practice as MC and MG methods. In actual construction sites, especially open-cut sites, GNSSs may be unusable and struts or existing structures may obstruct optical signals, compromising MG/MC implementation. In addition, construction management is difficult because only the operator can view the MG/MC screen, so site staff cannot confirm the construction status in real time. A potential solution is to measure the excavation surface directly using dense point

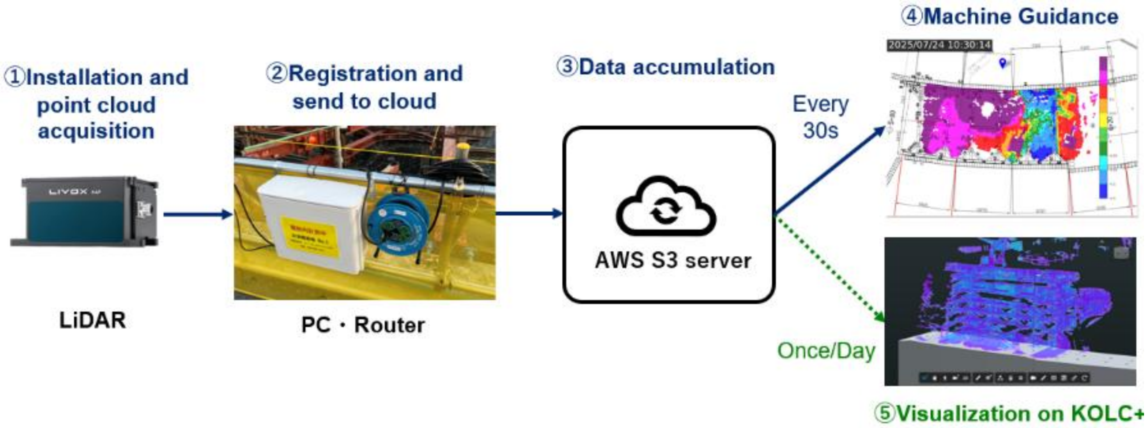

Figure 1. System configuration

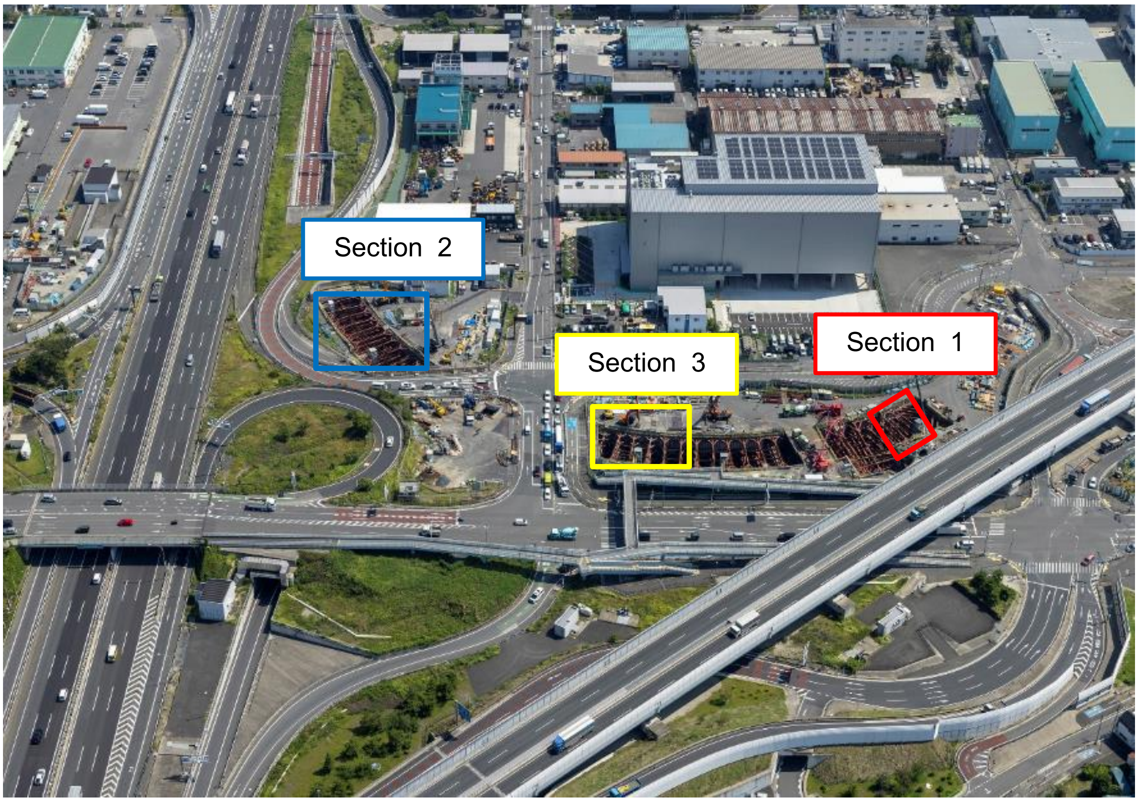

Figure 1. Tokyo Gaikan Expressway Keiyo Junction G ramp

cloud data obtain from 3D LiDAR (hereinafter "LiDAR") and transmit the data to the cloud in real time instead of estimating machine posture by tracking prisms. Although previous studies have proposed point cloud registration methods utilizing feature points and BIM, there are very few examples of these methods being applied to MG or autonomous construction [5]–[7]. Because point cloud registration may fail in feature-poor sites, such as tunnels, we propose a method for transforming point clouds from multiple LiDARs into the site coordinate system using a jig and TS measurements. We constructed a point cloud measurement system using this method in an actual open-cut tunnel site and performed measurements. This paper describes the proposed system and the evolution of measurement conditions.

2 System Configuration and Site Overview

Figure 1 illustrates the configuration of the proposed system. It comprised a LiDAR (Livox HAP [8]) for point cloud measurement, a PC (ASUS NUC) for data processing, and a Power over Ethernet hub and mobile router for data transmission to the cloud (AWS S3 server). The field of view of the LiDAR was 120° (horizontal) × 25° (vertical), and its detection range was 150 m. The system was installed at the Tokyo Gaikan Expressway Keiyo Junction G ramp construction site in Ichikawa City, Chiba Prefecture. In this open-cut tunnel construction site, excavation proceeds within diaphragm walls supported by struts. Figure 2 presents an overview photograph of the site. Measurements were conducted at three locations (Sections 1–3) according to the construction progress. The basic system configuration was consistent across all measurements, but the LiDAR installation and registration methods differed slightly between sections, as described in the subsequent subsections.

Figure 3. LiDAR and type I jig

3 Measurement Method and Result

3.1 Measurement in Section 1

Figure 4. LiDAR installation in Section 1

Measurements in Section 1 were conducted in July 2024. Point clouds were acquired using three LiDAR units (#110, #111, and #113) installed within an area of approximately 10 m × 10 m. Figure 3 shows the appearance of the LiDAR and the jig (type 1), and Figure 4 shows the LiDAR installation status. The LiDAR-obtained point clouds, which were in a local coordinate system centered on the LiDAR's optical origin, were transformed into the survey coordinate system. Mainstream methods for point cloud registration, such as RANSAC and ICP matching [9][10], estimate LiDAR position and orientation based on feature points. However, construction sites commonly have identical, equally spaced pillars or feature-poor environments, such as in tunnels.

We address this problem using the method illustrated in Figure 5. First, the TS instrument point was determined using prisms #1-1 and #1-2, which were placed at two or more known points. Next, three or more prisms or reflective sheets (#2-1 to #2-3) attached to the jig were measured in the site coordinate system. Finally,

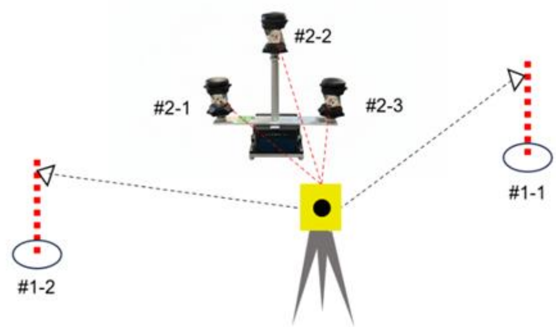

Figure 5. LiDAR position estimation

we estimated the LiDAR's optical origin and yaw, pitch, and roll angles by calculating the rigid-body transformation matrix required to align the coordinates of the prisms on the jig. Rigid-body transformations were used to determine the LiDAR origin and orientation from the three prisms. Let p_i denote the coordinates of the three prisms in the LiDAR coordinate system (where i is the prism number; i = 1, 2, 3), and let q_i denote the coordinates of the prisms in the common coordinate system. The relationship between p_i and q_i is given by Equation (1):

$$q_i = Rp_i + t \quad (1)$$

where R is a 3 × 3 rotation matrix and t is the translation vector of the LiDAR origin. R is obtained using the covariance matrix and singular value decomposition; further details are available in a previous study [11].

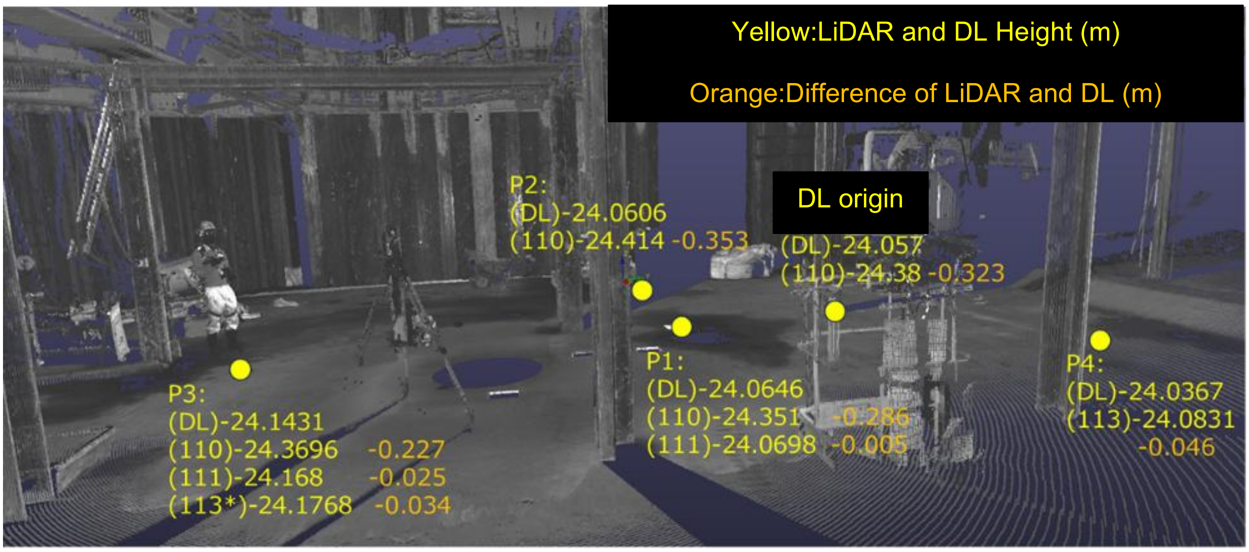

Figure 6. LiDAR and DL heights

From the obtained rotation matrix *R*, quaternions were calculated and the roll, pitch, and yaw angles were estimated [12][13]. Figure 6 compares the height of the acquired point cloud with the height measured by a digital level. The background in Figure 6 was obtained using a terrestrial laser scanner. The error was ~5 mm in high-accuracy areas but reached 400 mm in others. The excavation depths at this site were currently monitored at fixed points approximately 10 m × 5 m grids with ±50 mm accuracy by level gauge, and similar or higher accuracy and resolution were expected from the MG system. The TS used for prism surveying (TOPCON GT-1003) had an error of 2.1 mm when measuring distances in the nonprism mode from 50 m away; hence, the LiDAR origin and orientation were calculated using coordinate values incorporating this error. Therefore, each coordinate in Equation (1) contained this error, potentially causing position and orientation estimation errors. Furthermore, for example, acquiring point clouds from a distance of 10 m with an accuracy of 20 mm or less requires an accuracy of 2/1000 ~ 0.11° or less. Consequently, the coordinate values of the prism, which were in millimeters, would not have enabled angle estimation with the necessary precision. Given the difficulty of estimating the LiDAR position and angle solely using the prisms attached to the jig, we concluded that sufficient MG/MC would not be feasible under these conditions.

Furthermore, installing the LiDAR at a near-horizontal angle relative to the ground surface resulted in significant point cloud occlusion by obstacles and required frequent adjustments to the device angle and position as the excavation deepened. Therefore, we explored an installation method that would enable continuous measurement of the same area to the greatest extent possible.

3.2 Measurement in Section 2

Measurements in Section 2 were conducted from November 2024 to August 2025. The measurement area was approximately 10 m wide and 30 m long. One LiDAR unit was installed between each strut, for a total of seven units (#1–#7). For LiDARs #1–#5, the fabricated aluminum frame jig (type 2) differed from that in Section 1. Figure 7 shows this LiDAR jig, and Figure 8 shows the LiDAR installation status. The measurement coverage in Section 2 was improved relative to that in Section 1 by positioning the LiDAR near ground level and directing it toward the excavation surface; in Section 1, it was placed at a near-horizontal angle near the excavation surface.

For point cloud registration, in addition to calculating the LiDAR position and orientation from three or more prisms or reflective sheets (Section 1), we placed reflective sheets on the excavation surface during installation and measured their coordinates using a TS. We then fine-tuned the numerical values such that the LiDAR and TS-measured coordinates matched. Figure 9 illustrates the fine-tuning of the LiDAR orientation. The measured point cloud data were processed using a PC installed inside an on-site distribution board and transmitted to the cloud via an LTE connection. When performing MG, it is necessary to display point clouds of the excavation surface to the operator in real time and with the highest possible resolution. However, attempting to display the point cloud data as is presents challenges such as noise in the point clouds and the sheer volume of data. For this system, field construction staff requested a resolution of 250-mm intervals and a refresh rate of 30 s or less. Therefore, rather than displaying the point cloud data directly, we decided to accumulate the measured point cloud data within a 250-mm square grid for 30 s and display the average value, resolving the issues of point cloud noise and data transmission volume. The cloud data were visualized as contours and displayed on tablets in the heavy machinery operator's cab and on monitors in the site office every 30 s. Additionally, LAS data were uploaded to the cloud once a day for viewing in KOLC+ [14], balancing utility for MG/MC and convenience for daily construction management. Figure 10 shows the MG screen, and Figure 11 shows the visualization in KOLC+. Parts of the area are occluded by elements such as the horizontal struts. Figure 12 shows the progress of the final excavation in the measured area. The contours represent the difference between the measured data and the BIM model data; purple indicates high areas, yellow-green/green indicates areas within the control values, and blue indicates low areas. Evidently, the excavation surface lowers over time. Additionally, some areas appear high due to temporary soil stockpiles or heavy machinery. Activities occurring in parallel with excavation, such as the spreading of crushed stone, are also visible.

Regarding measurement accuracy, Figures 13 and 14 show a comparison of LiDAR and TS data, which was conducted during LiDAR installation, and a histogram of the errors relative to the TS data (data for #5 and #7 are missing), respectively. The errors were generally approximately ±20 mm, falling within 40 mm at most. For #6 and #7, relatively larger errors likely occurred because the jig was the same as in Section 1 and the installation dates were different. LiDAR accuracy may have varied due to the irradiation distance, strut displacement, and vibrations caused by the heavy machinery or wind. Moreover, manual fine-tuning was time consuming, and registration accuracy relied on operator subjectivity. These limitations highlighted the need for a method that would determine positions and angles with high precision, eliminating operator dependence.

Figure 7. LiDAR and type 2 jig

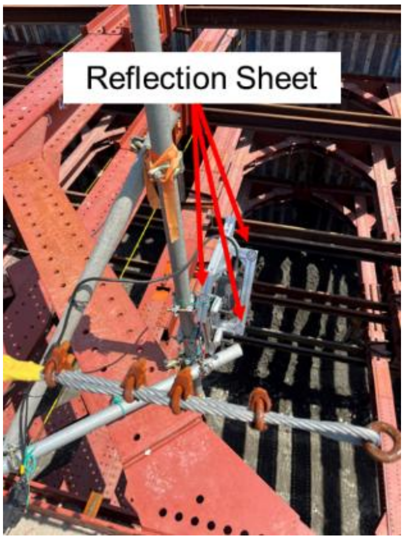

Figure. 8. LiDAR installation LiDAR in Section 2

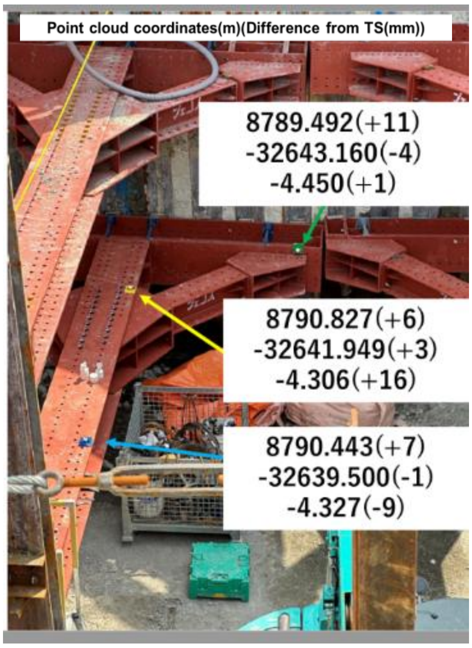

Figure 9. Adjusting of LiDAR position

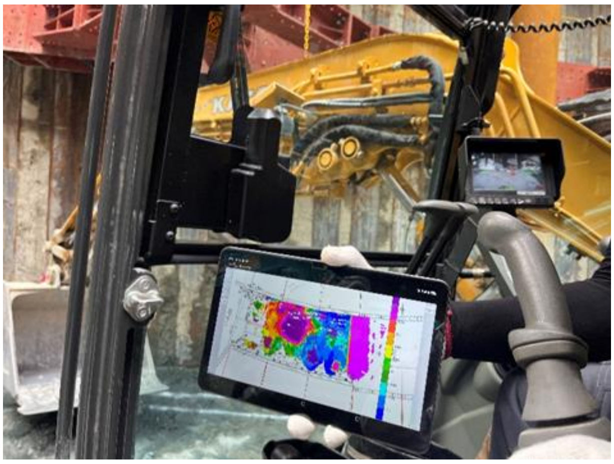

Figure 10. MG display

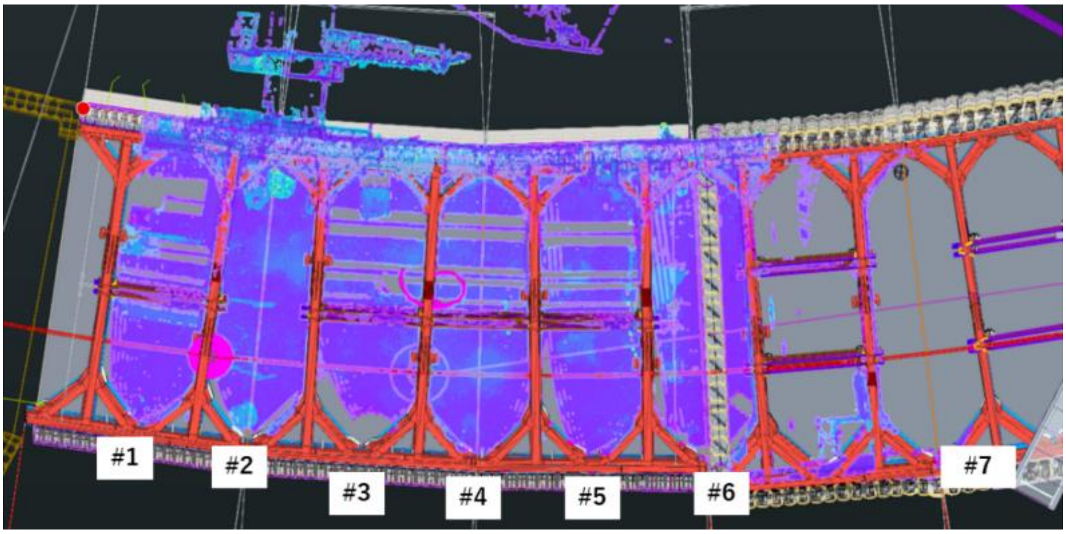

Figure 11. Point cloud visualization in KOLC+

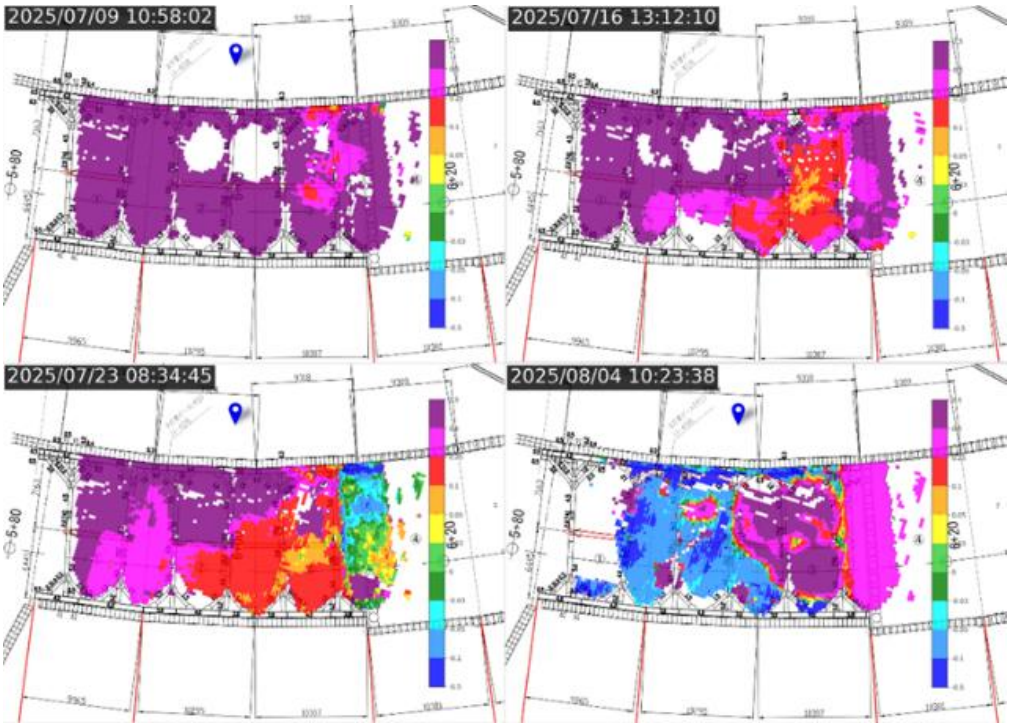

Figure 12. Progress of excavation

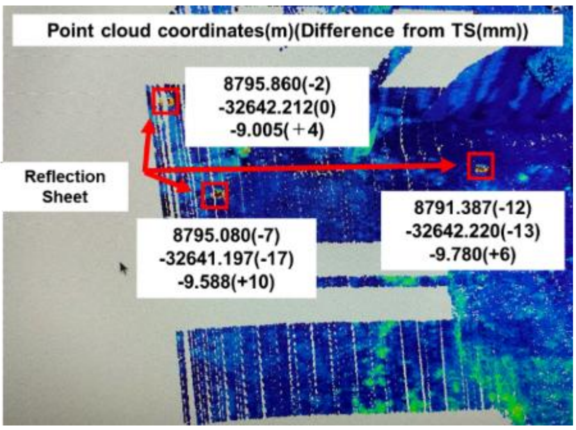

Figure 13. Accuracy verification

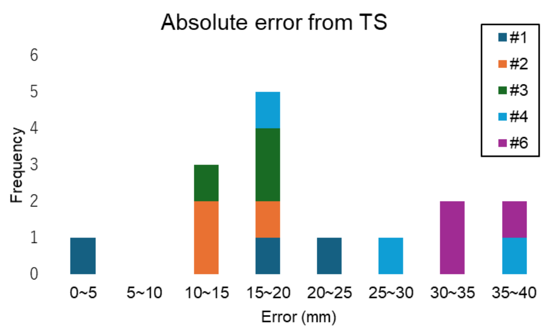

Figure. 14. Error histogram

3.3 Measurement in Section 3

Measurements were performed in Section 3 from October 2025 to January 2026. In Section 2, workability problems occurred due to the placement of reflective sheets on the excavation surface during installation to fine-tune the LiDAR orientation based on their coordinates. Therefore, we fabricated a type 3 jig (Figure 15) from sheet metal. It had a tribrach at the bottom, a circular bubble level on top, and two reflective sheets attached to its top and side. The roll and pitch angles were precisely set to 90° and 45°, respectively, by leveling the jig using the bubble level. Once the coordinates of the two reflective sheets were determined, the LiDAR's optical origin and yaw angle were calculated. The origin and angles (X, Y, Z, θ, φ, γ) of this LiDAR are expressed as shown in Equation (2) using the coordinates (X_1, Y_1, Z_1) of the upper reflective sheet and the coordinates (X_2, Y_2, Z_2) of the lateral reflective sheet.

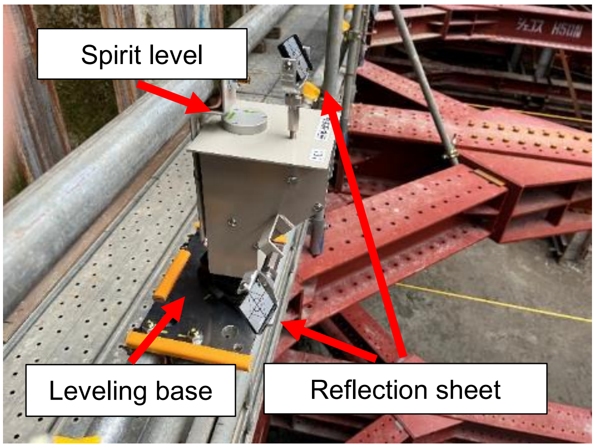

Figure 15. LiDAR and type 3jig

$$X = X_1 - 0.005\ sin\gamma$$
$$Y = Y_1 - 0.005\ cos\gamma$$
$$Z = Z_2 - 0.005,$$
$$\theta = -\frac{\pi}{2} \quad (2)$$
$$\varphi = \frac{\pi}{4}$$
$$\gamma = atan2((Y_2 - Y_1), (X_2 - X_1)).$$

An example of the results is shown in Figure 16. Without manual fine-tuning, the height was generally within 20 mm, but the error exceeded 100 mm in the planar direction. This large error may have been resulted from the difficulty of determining the yaw angle using a prism (Section 3.1). In future, we plan to investigate methods for estimating yaw angles without using a prism.

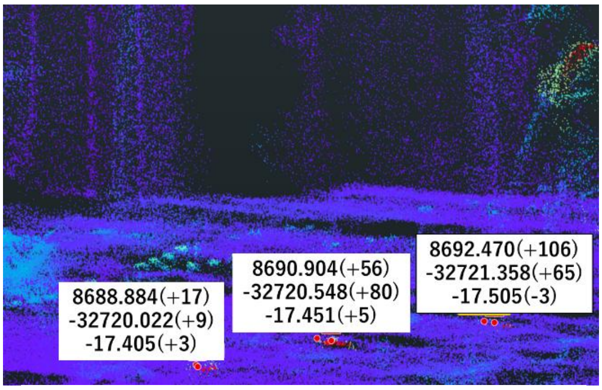

Figure 16. Accuracy verification of type-3 jig

4 Discussion and Future Work

Unlike conventional registration methods in general robotics applications, point cloud registration often relies on feature-based matching algorithms, such as RANSAC and ICP [6][7]. However, the environments in open-cut tunnel construction sites have repetitive geometric features (e.g., equally spaced earth-retaining struts) and feature-poor surfaces (e.g., flat excavation bottoms or shotcrete walls). In such environments, conventional algorithms tend to fall into local minima, leading to significant registration errors. Furthermore, construction management requires not only relative-map merging but also transformation of point clouds into the absolute site coordinate system for comparisons with BIM model data. Our proposed method, which utilizes a jig and TS measurements, ensures robust point cloud transformation into the site coordinate system, regardless of the geometric features of the environment. This reliability is a critical requirement for practical construction management and MG.

The measurement results from Sections 1 and 2 highlighted the significant impact of LiDAR installation geometry on measurement accuracy. In Section 1, the LiDAR was installed at a low position, at a near-horizontal incidence angle relative to the excavation surface. This configuration caused two issues: (1) significant occlusion by obstacles due to the shallow angle and (2) frequent adjustment of the LiDAR angle with each excavation step. By contrast, the setup in Section 2, where the LiDARs were mounted facing downward on the struts, minimized occlusions and ensured a high incidence angle. The achieved accuracy of approximately ±20 mm in Section 2 satisfied the general tolerance for rough excavation, confirming the system's applicability to MG.

The primary challenge identified in Section 2 was the operational complexity of fine-tuning. This method required installing three or more reflective sheets on the excavation surface and performing labor-intensive calculations of the rigid-body transformation matrix, either manually or via programming, which disrupted construction activities. The type 3 jig addressed this issue by incorporating the bubble level and the fixed tribrach. By mechanically constraining the roll and pitch angles to known values (leveling), we simplified the positioning problem to determining only the translation and yaw angle. This improvement will significantly reduce installation times and eliminate the need to access the excavation floor, thereby enhancing safety and operational efficiency.

Static accuracy was verified while the system operated in a dynamic environment. The slight errors observed in Section 2 (Figures 13 and 14) may be attributed to sensor noise and strut vibration caused by heavy machinery and the minute displacement of the struts over time. Because the LiDAR was mounted on the struts, any shoring deformation directly affected the point cloud coordinates. Future work must distinguish between sensor registration errors and actual structural displacement to utilize this system for the safety monitoring of earth-retaining walls.

5 Conclusion

This study proposes a practical LiDAR-based MG system designed for open-cut tunnel excavation sites, where GNSS signals may be unavailable and geometric features are repetitive. By integrating multiple LiDAR sensors with a TS using a specialized registration jig, we established a workflow for accurately transforming point cloud data into the absolute site coordinate system.

Our field trials demonstrated the critical importance of sensor placement and registration method. The initial trial (Section 1) suffered from occlusion and a low incidence angle, but the improved setup in Section 2—with the LiDARs mounted vertically on earth-retaining struts—achieved a measurement accuracy of approximately ±20 mm. This accuracy is well within the tolerance required for excavation, validating the system's effectiveness for real-time MG. Furthermore, the development of the leveling-enabled (type 3) jig addresses the operational bottleneck of manual fine-tuning, offering a solution that significantly reduces installation time and labor costs.

In conclusion, the proposed system enables precise construction management in environments with limited features. Furthermore, it enhances safety and facilitates efficient site management by minimizing the need for site foremen to enter excavation areas. Future research will verify the efficiency of the type 3 jig in ongoing projects and investigate its potential application to other measurements, such as those involved in concrete placement and the structural displacement monitoring of retaining walls, contributing to comprehensive site safety management.

References

[1] MLIT. I-construction 2.0. Online: https://www.mlit.go.jp/tec/constplan/content/001738240.pdf, Accessed: 26/12/2025.

[2] R. Heikkila and M. Jaakkola. Automation of road construction - the state of the art in Europe. In Proceedings of the 23rd International Symposium on Automation and Robotics in Construction (ISARC2006), pages 7–10, Tokyo, Japan, 2006

[3] T. Hachijo, et al. 3D measurement system for soil loading by an autonomous backhoe using OPERA. In Proceedings of the 42nd International Symposium on Automation and Robotics in Construction (ISARC2025), pages 1501–1506, Montreal, Canada, 2025

[4] KOMATSU. 3D machine guidance. Online: https://www.komatsu.com/en-us/technology/smart-construction/3d-machine-guidance, Accessed: 26/12/2025.

[5] Y. Zhang, L. Lu, X. Luo, and J. Pan. Global BIM-point cloud registration and association for construction progress monitoring. Automation in Construction, Vol. 168, Part A, 105796, 2024.

[6] Z. Xu, B. Schwab, Y. Yang, T. H. Kolbe, and C. Holst. L2M-Reg: Building-level uncertainty-aware registration of outdoor LiDAR point clouds and semantic 3D city models. ISPRS Journal of Photogrammetry and Remote Sensing, Vol. 233, pages 467–486, 2026.

[7] J. Kim, J. Kim, S. Paik, and H. Kim. Point cloud registration considering safety nets during scaffold installation using sensor fusion and deep learning. Automation in Construction, Vol. 159, 105277, 2024.

[8] Livox Technology Company Limited. LIVOX HAP. Online: https://www.livoxtech.com/jp/hap, Accessed: 26/12/2025.

[9] M. Fischler and R. Bolles. Random sample consensus: a paradigm for model fitting with application to image analysis and automated cartography. Communications of the ACM, Vol. 24, No. 6, pp. 381–395, 1981.

[10] J. Paul and N. D. McKay. A method for registration of 3-D shapes. IEEE Transactions Pattern Analysis and Machine Intelligence, Vol. 14, No. 2, pp. 239–256, 1992.

[11] K. S. Arun, T. S. Huang, and S. D. Blostein. Least-squares fitting of two 3-D point sets. IEEE Transactions on Pattern Analysis and Machine Intelligence, Vol. PAMI-9, No. 5, pages 698–700, 1987.

[12] SciPy. Online: https://docs.scipy.org/doc/scipy/reference/generated/scipy.spatial.transform.Rotation.from_matrix.html#id3, Accessed: 24/3/2026.

[13] F. L. Markley. Unit quaternion from rotation matrix. Journal of Guidance, Control, and Dynamics, Vol. 31.2, pp. 440–442, 2008.

[14] KOLG Inc. KOLC+ BIM/CIM sharing cloud. Online: https://kolcx.com/, Accessed: 26/12/2025.